Rui Li[1]
State Key Laboratory of Structural Analysis for Industrial Equipment,
Department of Engineering Mechanics, and International Research Center for Computational Mechanics,
Dalian University of Technology,
Dalian 116024, China;
State Key Laboratory of Digital Manufacturing Equipment and Technology,
Huazhong University of Science and Technology,
Wuhan 430074, China
e-mail: ruili@dlut.edu.cn

Pengcheng Wang
State Key Laboratory of Structural Analysis for Industrial Equipment,
Department of Engineering Mechanics, and International Research Center for Computational Mechanics,
Dalian University of Technology,
Dalian 116024, China

Bo Wang
College of Engineering,
Peking University,
Beijing 100871, China

Chunyu Zhao
CAS Key Laboratory of Mechanical Behavior and Design of Materials,
Department of Modern Mechanics,
University of Science and Technology of China,
Hefei 230027, China

Yewang Su[1]
State Key Laboratory of Nonlinear Mechanics,
Institute of Mechanics,
Chinese Academy of Sciences,
Beijing 100190, China;
School of Engineering Science,
University of Chinese Academy of Sciences,
Beijing 100049, China
e-mail: yewangsu@imech.ac.cn

New Analytic Free Vibration Solutions of Rectangular Thick Plates With a Free Corner by the Symplectic Superposition Method

Seeking analytic free vibration solutions of rectangular thick plates without two parallel simply supported edges is of significance for an insight into the performances of related engineering devices and structures as well as their rapid design. A challenging set of problems concern the vibrating plates with a free corner, i.e., those with two adjacent edges free and the other two edges clamped or simply supported or one of them clamped and the other one simply supported. The main difficulty in solving one of such problems is to find a solution meeting both the boundary conditions at each edge and the condition at the free corner, which is unattainable using a conventional analytic method. In this paper, for the first time, we extend a novel symplectic superposition method to free vibration of rectangular thick plates with a free corner. The analytic frequency and mode shape solutions are both obtained and presented via comprehensive numerical and graphic results. The rigorousness in mathematical derivation and rationality of the method (without any predetermination for the solutions) guarantee the validity of our analytic solutions, which themselves are also validated by the reported results and refined finite element analysis. [DOI: 10.1115/1.4038951]

Keywords: thick plate, free corner, free vibration, analytic solution, symplectic superposition method

1 Introduction

Solving the free vibration problems of plate structures has been an important topic in mechanical engineering, which is very useful for the performance analysis and design of related engineered devices and structures. Although many progresses have been gained in seeking the solutions of plates with various shapes, as summarized in Leissa's seminal monograph [1], analytic solutions are far from complete due to the mathematical challenge in treating the plate models such as the Kirchhoff thin plate and more complex Mindlin/Reissner thick plate [2,3] or the others [4,5]. Conventional approximate/numerical methods include the finite element method (FEM), finite difference method, Rayleigh–Ritz method, Galerkin method, series method, etc. The reader is referred to Leissa's work [1] for more details, where comprehensive results are available for vibration of thin plates.

Many recently developed novel numerical methods have been explored for plates' vibration problems. Some representative methods are briefly reviewed in the following. Wu and Zhu [6] developed a new global spatial discretization method to accurately calculate natural frequencies and dynamic responses of two-dimensional continuous systems such as membranes and thin plates, where much fewer degrees-of-freedom and much less computational effort are needed compared with the FEM and finite difference method. Wang [7] presented the frequencies and mode shapes for the rounded rectangular thin plate with completely free edges by using a family of homotopy shapes with low powers, which greatly facilitate differentiation and numerical integrations for an efficient Ritz method. Leamy [8] proposed a phase closure approach for finding semi-exact, closed-form expressions for the natural frequencies of thin rectangular plates; the approach has the advantage of yielding highly accurate, closed-form algebraic expressions suitable for archiving in compilations such as

[1]Corresponding authors.
Contributed by the Technical Committee on Vibration and Sound of ASME for publication in the Journal of Vibration and Acoustics. Manuscript received September 10, 2017; final manuscript received January 4, 2018; published online February 9, 2018. Assoc. Editor: Izhak Bucher.

handbooks and manuals. Waksmanski et al. [9] obtained an exact closed-form solution for free vibration of a simply supported and multilayered one-dimensional quasi-crystal plate by using the pseudo-Stroh formulation and propagator matrix method; the work is very useful for further expanding the applications of quasi-crystal, especially when used for composite materials. Lai and Xiang [10] applied the discrete singular convolution method to investigate the buckling and vibration of heavy standing thin plates and obtained accurate first-known vibration solutions for elastically restrained vertical plates subjecting to body forces/self-weight. Besides, Malekzadeh and Karami [11] presented a differential quadrature procedure for free vibration analysis of moderately thick plates with variable thickness on two-parameter elastic foundations under in-plane edge forces; accurate results were obtained for higher-order modes of vibration with only few grid points, which demonstrates the advantage of low computation cost of the method. Cho et al. [12] applied the assumed mode method and mode superposition method to develop a very simple, fast, and accurate procedure for the forced vibration analysis of plates and stiffened panels, which is especially appropriate for early design stage when different dimensions of plates and stiffened panels and their influence on dynamic response are examined. In addition to these, the Rayleigh–Ritz method is still popular as a very efficient way to handle plates' vibration problems. The updates on the method focus on the selection of some novel admissible functions, yielding different expressions of displacement components. For example, Zhou et al. [13] utilized the admissible functions comprising the Chebyshev polynomials multiplied by a boundary function for free vibration analysis of rectangular plates with any thicknesses. Pradhan et al. [14] expressed the trial functions as the linear combinations of simple algebraic polynomials to study free vibration of thick rectangular plates based on new inverse trigonometric shear deformation theories. Ye et al. [15] adopted a new form of trigonometric series expansion to develop a modified Fourier solution for the free vibration problems of moderately thick rectangular plates based on the first-order shear deformation theory. Similar treatments were applied by Jin et al. [16] to obtain three-dimensional solution for the free vibrations of arbitrarily thick functionally graded rectangular plates, and by Zhang et al. [17] for the free vibration analysis of moderately thick rectangular plates with non-uniform boundary conditions.

In comparison with the numerous numerical methods, analytic approaches to plates' vibration problems are much fewer. For rectangular plates, it is known that the conventional semi-inverse Lévy method is only applicable to those having at least two parallel simply supported edges. Although some successful attempts have been made in recent years on obtaining the analytic solutions of intractable rectangular thin plate problems, including bending, vibration, and buckling of plates without two parallel simply supported edges [18–20], there have been rare reports for analytic vibration solutions of thick plates. Few available achievements are found for rectangular thick plates with only clamped and/or simply supported edges, as reported by Xing and Liu [21,22], or for plates with only one free edge, as reported by Li et al. [23]. The free vibration of rectangular thick plates with a free corner, i.e., with two adjacent edges free and the other two edges clamped or simply supported or one of them clamped and the other one simply supported, have not been solved analytically. The problems of this type are very interesting because not only the free edges but also the free corner is involved, whose analytic solutions are, however, very difficult to acquire due to the predicament in finding a solution meeting both the boundary conditions at each edge and the condition at the free corner. Therefore, seeking a novel analytic method becomes indispensable to settle these problems.

In recent years, a symplectic elasticity approach has been proposed by Yao et al. [24]. Compared with the classic analytic approaches such as the semi-inverse method, the symplectic approach is conducted in the Hamiltonian system, in physics, and in the symplectic space, in mathematics. Some useful techniques, such as the separation of variables that is sometimes invalid in the Euclid space, become valid in the symplectic space, which makes it possible to explore newer analytic solutions. The approach has been extended to many fields [25], among which the plate problems were further advanced by Lim et al. [26,27] and Li et al. [18,19,23,28]. In this paper, we obtain the analytic free vibration solutions of rectangular thick plates with a free corner by an elegant symplectic superposition method, which combines the rationality of the symplectic elasticity approach and generality of the superposition method such that the focused problems could be solved in a rigorous way, without any trial solutions predetermined. In the following, we first construct a fundamental free vibration problem, i.e., a vibrating plate with two adjacent edges slidingly clamped and the other two edges simply supported. With the Hamiltonian system-based variable separation in the symplectic space, which triggers an eigenvalue problem, and the symplectic eigen expansion, the analytic solution of the fundamental problem is obtained. By superposition of two fundamental solutions followed by its equivalence with the original problem, the equation for determining the natural frequencies is achieved. The mode shape associated with a frequency solution is then readily obtained. Comprehensive numerical and graphic results are provided for the plates under consideration, which offer the benchmarks for various emerging solution methods.

2 Fundamental Free Vibration Problem With Solution in the Symplectic Space

In a recently published study [23], we have constructed the governing equations of a Mindlin theory-based thick plate's free vibration in the symplectic space in the rectangular coordinate system *xoy* (Fig. 1(*a*)), which yields a Hamiltonian system-based matrix-form expression, written by

$$\partial \mathbf{Z}/\partial y = \mathbf{H}\mathbf{Z} \tag{1}$$

where

$$\mathbf{Z} = [\Phi, w, \Psi, \alpha, \beta, \theta]^{\mathrm{T}} \tag{2}$$

is the state vector, incorporating the modal displacement w and five other functions, i.e., Φ, Ψ, α, β, and θ, defined by

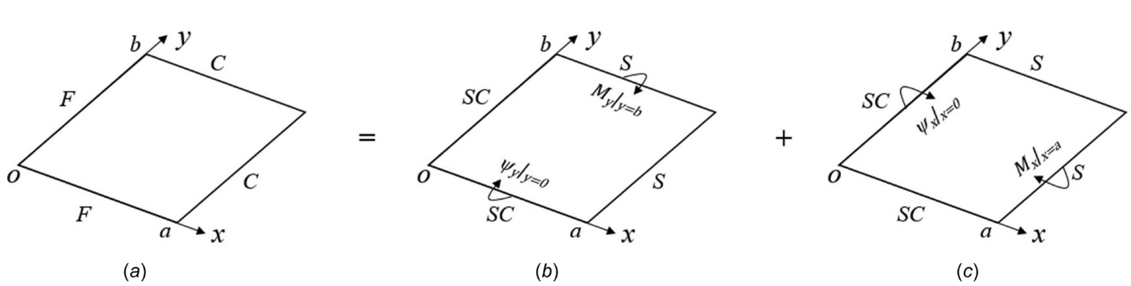

Fig. 1 Symplectic superposition for free vibration of a CCFF thick plate

$$\Phi = \frac{\partial \psi_x}{\partial x} + \frac{\partial \psi_y}{\partial y} \tag{3}$$

$$\Psi = \frac{\partial \psi_y}{\partial x} - \frac{\partial \psi_x}{\partial y} \tag{4}$$

$$\alpha = \frac{D}{\rho h \omega^2}\frac{\partial \Phi}{\partial y} \tag{5}$$

$$\beta = \frac{\partial w}{\partial y} \tag{6}$$

and

$$\theta = \frac{\partial \Psi}{\partial y} \tag{7}$$

Here, ψ_x and ψ_y denote the rotating angles about the y- and x-axes, respectively; ρ is the mass density of plate, h the thickness, ω the natural frequency, and D the flexural stiffness. The Hamiltonian matrix $\mathbf{H}$ has the form

$$\mathbf{H} = \begin{bmatrix} \mathbf{0} & \mathbf{F} \\ \mathbf{G} & \mathbf{0} \end{bmatrix} \tag{8}$$

with

$$\mathbf{F} = \begin{bmatrix} \rho h \omega^2/D & 0 & 0 \\ 0 & 1 & 0 \\ 0 & 0 & 1 \end{bmatrix} \tag{9}$$

and

$$\mathbf{G} = \begin{bmatrix} -\frac{D}{\rho h \omega^2}\frac{\partial^2}{\partial x^2} & 1 & 0 \\ 1 & -\frac{\partial^2}{\partial x^2} - \frac{\rho h \omega^2}{C} & 0 \\ 0 & 0 & \frac{10}{h^2} - \frac{\partial^2}{\partial x^2} \end{bmatrix} \tag{10}$$

where C is the shear stiffness. If Eq. (1) is successfully solved, the key quantities for a thick plate's free vibration can be readily obtained via w, Φ, and Ψ. For example, besides w, the other two general modal displacements ψ_x and ψ_y are obtained by

$$\begin{aligned} \psi_x &= \frac{\partial w}{\partial x} + \frac{D}{C}\left[\frac{\partial \Phi}{\partial x} - \frac{1-\nu}{2}\frac{\partial \Psi}{\partial y}\right] \\ \psi_y &= \frac{\partial w}{\partial y} + \frac{D}{C}\left[\frac{\partial \Phi}{\partial y} + \frac{1-\nu}{2}\frac{\partial \Psi}{\partial x}\right] \end{aligned} \tag{11}$$

Then all other quantities can be obtained, e.g., the bending moments $M_x = -D(\partial\psi_x/\partial x + \nu\partial\psi_y/\partial y)$ and $M_y = -D(\partial\psi_y/\partial y + \nu\partial\psi_x/\partial x)$, twisting moment $M_{xy} = -D(1-\nu)(\partial\psi_x/\partial y + \partial\psi_y/\partial x)/2$, shear forces $Q_x = C(\partial w/\partial x - \psi_x)$ and $Q_y = C(\partial w/\partial y - \psi_y)$, with ν as the Poisson's ratio. Therefore, w, Φ, and Ψ are regarded as the governing functions in the present solution system. The main advantage of the description in the symplectic space via the Hamiltonian system-based governing equation (1) is the applicability of some powerful mathematical techniques such as the separation of variables and symplectic eigen expansion, which are not necessarily attainable in the Euclidean space [24]. As a result, seeking the analytic solutions to some complex problems becomes probable.

For free vibration of the plates with a free corner, constructing a fundamental problem is necessary in the symplectic superposition method. As shown in Fig. 1(*b*), we first investigate a plate slidingly clamped at $x = 0$ and simply supported at $x = a$, with a rotating angle $\psi_y|_{y=0}$ and a bending moment $M_y|_{y=b}$ imposed at the slidingly clamped edge $y = 0$ and the simply supported edge $y = b$, respectively. The boundary conditions of the plate are

$$\begin{aligned} \psi_x|_{x=0} = 0, \quad Q_x|_{x=0} = 0, \quad M_{xy}|_{x=0} = 0 \\ w|_{x=a} = 0, \quad \psi_y|_{x=a} = 0, \quad M_x|_{x=a} = 0 \end{aligned} \tag{12}$$

and

$$\begin{aligned} \psi_y|_{y=0} = \sum_{m=1,3,5,\ldots}^{\infty} E_m \cos(\alpha_m x), \quad Q_y|_{y=0} = 0, \quad M_{xy}|_{y=0} = 0 \\ w|_{y=b} = 0, \quad \psi_x|_{y=b} = 0, \quad M_y|_{y=b} = \sum_{m=1,3,5,\ldots}^{\infty} F_m \cos(\alpha_m x) \end{aligned} \tag{13}$$

where $\psi_y|_{y=0}$ and $M_y|_{y=b}$ are expressed by the Fourier expansion, with $\alpha_m = m\pi/(2a)$ and the constants E_m and F_m $(m = 1, 3, 5, \ldots)$ to be determined later. A similar fundamental problem is shown in Fig. 1(*c*), where the plate is slidingly clamped at $y = 0$ and simply supported at $y = b$, with a rotating angle $\psi_x|_{x=0}$ and a bending moment $M_x|_{x=a}$ imposed at the slidingly clamped edge $x = 0$ and the simply supported edge $x = a$, respectively. The boundary conditions are

$$\begin{aligned} \psi_y|_{y=0} = 0, \quad Q_y|_{y=0} = 0, \quad M_{xy}|_{y=0} = 0 \\ w|_{y=b} = 0, \quad \psi_x|_{y=b} = 0, \quad M_y|_{y=b} = 0 \end{aligned} \tag{14}$$

and

$$\begin{aligned} \psi_x|_{x=0} = \sum_{m=1,3,5,\ldots}^{\infty} G_m \cos(\beta_m y), \quad Q_x|_{x=0} = 0, \quad M_{xy}|_{x=0} = 0 \\ w|_{x=a} = 0, \quad \psi_y|_{x=a} = 0, \quad M_x|_{x=a} = \sum_{m=1,3,5,\ldots}^{\infty} H_m \cos(\beta_m y) \end{aligned} \tag{15}$$

where $\beta_m = m\pi/(2b)$, G_m and H_m $(m = 1, 3, 5, \ldots)$ are the constants to be determined. It is found that the second problem (Fig. 1(*c*)) is actually the same as the first one (Fig. 1(*b*)) after the coordinates exchange. Therefore, only the first fundamental problem needs to be solved.

In the symplectic space, the separation of variables is valid [24], which implies that $\mathbf{Z} = \mathbf{X}(x)\,Y(y)$ can be applied to Eq. (1). yielding $\mathrm{d}Y(y)/\mathrm{d}y = \mu Y(y)$ and $\mathbf{H}\mathbf{X}(x) = \mu\mathbf{X}(x)$, where $\mathbf{X}(x) = [\Phi(x), w(x), \Psi(x), \alpha(x), \beta(x), \theta(x)]^{\mathrm{T}}$ is the eigenvector, with μ as the eigenvalue. Combining the boundary conditions expressed in Eq. (12), we derive the eigenvalues

$$\begin{aligned} \mu_{\pm m}^{(1)} &= \pm\sqrt{\alpha_m^2 - \bar{S}\bar{\omega}^2/a^2} \\ \mu_{\pm m}^{(2)} &= \pm\sqrt{\alpha_m^2 - \bar{R}\bar{\omega}^2/a^2} \\ \mu_{\pm m}^{(3)} &= \pm\sqrt{\alpha_m^2 + 10/h^2} \end{aligned} \tag{16}$$

and the associated eigenvectors

$$
\begin{aligned}
\mathbf{X}_{\pm m}^{(1)}(x) &= \left[\bar{R}\bar{\omega}^2\cos(\alpha_m x),\ a^2\cos(\alpha_m x),\ 0,\ \mu_{\pm m}^{(1)}\bar{R}a^4\cos(\alpha_m x),\ \mu_{\pm m}^{(1)}a^2\cos(\alpha_m x),\ 0\right]^{\mathrm{T}} \\
\mathbf{X}_{\pm m}^{(2)}(x) &= \left[\bar{S}\bar{\omega}^2\cos(\alpha_m x),\ a^2\cos(\alpha_m x),\ 0,\ \mu_{\pm m}^{(2)}\bar{S}a^4\cos(\alpha_m x),\ \mu_{\pm m}^{(2)}a^2\cos(\alpha_m x),\ 0\right]^{\mathrm{T}} \\
\mathbf{X}_{\pm m}^{(3)}(x) &= \left[0,\ 0,\ \sin(\alpha_m x),\ 0,\ 0,\ \mu_{\pm m}^{(3)}\sin(\alpha_m x)\right]^{\mathrm{T}}
\end{aligned} \tag{17}
$$

for $m = 1, 3, 5, \ldots$, where $\bar{\omega} = \omega a^2\sqrt{\rho h/D}$, $\bar{R} = (\delta - \sqrt{4/\bar{\omega}^2 + \delta^2})/2$, and $\bar{S} = (\delta + \sqrt{4/\bar{\omega}^2 + \delta^2})/2$, with $\delta = D/(\mathrm{C}a^2)$. The solution of Eq. (1) is written as

$$
\mathbf{Z} = \sum_{m=1,3,5,\ldots}^{\infty}\left[f_m^{(1)}\mathrm{e}^{\mu_m^{(1)}y}\mathbf{X}_m^{(1)}(x) + f_{-m}^{(1)}\mathrm{e}^{-\mu_m^{(1)}y}\mathbf{X}_{-m}^{(1)}(x) + f_m^{(2)}\mathrm{e}^{\mu_m^{(2)}y}\mathbf{X}_m^{(2)}(x) + f_{-m}^{(2)}\mathrm{e}^{-\mu_m^{(2)}y}\mathbf{X}_{-m}^{(2)}(x) + f_m^{(3)}\mathrm{e}^{\mu_m^{(3)}y}\mathbf{X}_m^{(3)}(x) + f_{-m}^{(3)}\mathrm{e}^{-\mu_m^{(3)}y}\mathbf{X}_{-m}^{(3)}(x)\right] \tag{18}
$$

where $f_{\pm m}^{(1)}$ to $f_{\pm m}^{(3)}$ $(m = 1, 3, 5, \ldots)$ are the constant coefficients, determined by substitution of the required quantities obtained by w, Φ, and Ψ from Eq. (18) into Eq. (13). The resultant solutions of the governing functions for the first fundamental problem, denoted by w_1, Φ_1, and Ψ_1, respectively, are

$$
\begin{aligned}
w_1 = a \times \sum_{m=1,3,5,\ldots}^{\infty} &\frac{\cos(m\pi\bar{x}/2)}{20\delta\xi_m\eta_m\bar{\omega}^2(\bar{R}-\bar{S})} \times \left\{\phi\{\epsilon_m\eta_m \mathrm{sech}\xi_m \mathrm{sh}[\xi_m(1-\bar{y})] - \zeta_m\xi_m \mathrm{sech}\eta_m \mathrm{sh}[\eta_m(1-\bar{y})]\}E_m\right. \\
&\left. + 20\delta\xi_m\eta_m\left[\mathrm{sech}\xi_m \mathrm{ch}(\xi_m\bar{y}) - \mathrm{sech}\eta_m \mathrm{ch}(\eta_m\bar{y})\right]\bar{F}_m\right\}
\end{aligned} \tag{19}
$$

$$
\begin{aligned}
\Phi_1 = \frac{1}{a} \times \sum_{m=1,3,5,\ldots}^{\infty} &\frac{\cos(m\pi\bar{x}/2)}{20\delta\xi_m\eta_m(\bar{R}-\bar{S})} \times \left\{\phi\left\{\bar{S}\epsilon_m\eta_m \mathrm{sech}\xi_m \mathrm{sh}[\xi_m(1-\bar{y})] - \bar{R}\xi_m\zeta_m \mathrm{sech}\eta_m \mathrm{sh}[\eta_m(1-\bar{y})]\right\}E_m\right. \\
&\left. + 20\delta\xi_m\eta_m(\bar{R}-\bar{S})\left[\bar{S}\mathrm{sech}\xi_m \mathrm{ch}(\xi_m\bar{y}) - \bar{R}\mathrm{sech}\eta_m \mathrm{ch}(\eta_m\bar{y})\right]\bar{F}_m\right\}
\end{aligned} \tag{20}
$$

and

$$
\Psi_1 = \frac{1}{a} \times \sum_{m=1,3,5,\ldots}^{\infty} \frac{m\pi \mathrm{sech}\gamma_m \sin(m\pi\bar{x}/2)}{5\delta\gamma_m(1-\nu)}\left\{5\delta\phi\, \mathrm{sh}(\gamma_m\bar{y})\bar{F}_m - \gamma_m\bar{h}^2 \mathrm{ch}[\gamma_m(1-\bar{y})]E_m\right\} \tag{21}
$$

where $\bar{x} = x/a$, $\bar{y} = y/b$, $\phi = b/a$, $\bar{F}_m = aF_m/D$, $\xi_m = \phi\sqrt{m^2\pi^2 - 4\bar{R}\bar{\omega}^2}/2$, $\eta_m = \phi\sqrt{m^2\pi^2 - 4\bar{S}\bar{\omega}^2}/2$, $\epsilon_m = m^2\pi^2\bar{h}^2 - 20\delta\bar{R}\bar{\omega}^2$, $\zeta_m = m^2\pi^2\bar{h}^2 - 20\delta\bar{S}\bar{\omega}^2$, and $\gamma_m = \phi\sqrt{40/\bar{h}^2 + m^2\pi^2}/2$, with $\bar{h} = h/a$. The coordinates exchange gives the solutions of the second fundamental problem (Fig. 1(*c*)) by replacing x, y, a, b, E_m, and F_m with y, x, b, a, G_m, and H_m, respectively.

3 Natural Frequency and Mode Shape Solutions by Superposition

For convenience, we use "S", "C", "F," and "SC" to stand for the simply supported, clamped, free and slidingly clamped edges, respectively. A clockwise four-letter symbolic notation is applied to a plate, with $y = b$ as the starting edge. The most complex free vibration problem of the rectangular thick plates with a free corner is for CCFF plate. It will be seen later that the other plates with a free corner, including CSFF and SSFF plates, can be treated as the special cases of CCFF plate when applying further simplifications. Superposition of the two fundamental solutions given in Sec. 2 constitutes the solution of a CCFF plate, as revealed in Fig. 1. However, there exist four sets of constants needing to be determined. To reach equivalence between Figs. 1(*a*) and 1(*b*) plus 1(*c*), the conditions that the following quantities vanish must be enforced: **(a)** superposition of M_y of the two fundamental problems at $y = 0$; **(b)** superposition of ψ_y at $y = b$; **(c)** superposition of M_x at $x = 0$; and **(d)** superposition of ψ_x at $x = a$. Corresponding to condition **(a)**, we have

$$
\begin{aligned}
&\left[\phi^2\left(\xi_i\zeta_i\bar{\epsilon}_i\,\mathrm{th}\,\eta_i - \eta_i\epsilon_i\bar{\zeta}_i\mathrm{th}\,\xi_i\right) + 4\delta\xi_i\eta_i\gamma_i i^2\pi^2\bar{h}^2\bar{\omega}^2\,\mathrm{th}\,\gamma_i(1-\nu)(\bar{R}-\bar{S})\right]E_i \\
&+ 20\delta\phi\xi_i\eta_i\left[\bar{\epsilon}_i\mathrm{sech}\eta_i - \bar{\zeta}_i\mathrm{sech}\xi_i + \delta i^2\pi^2\bar{\omega}^2\mathrm{sech}\gamma_i(1-\nu)(\bar{R}-\bar{S})\right]\bar{F}_i \\
&- \sum_{m=1,3,5,\ldots}^{\infty}\frac{32\phi\xi_i\eta_i\bar{\omega}^2(\bar{R}-\bar{S})}{\left(4\xi_i^2 + m^2\pi^2\right)\left(4\eta_i^2 + m^2\pi^2\right)\left[40\phi^2 + \pi^2\bar{h}^2\left(m^2 + i^2\phi^2\right)\right]} \\
&\times\left\{\left\{i^2\pi^2\phi^2\left\{4\delta\bar{R}\bar{S}\phi^2\bar{h}^2\bar{\omega}^4\left[20\nu\phi^2 - m^2\pi^2(1-\nu)\left(\bar{h}^2 - 5\delta\right)\right] + m^2\pi^2\left\{m^2\pi^2\bar{h}^4(1+\nu) - 4\phi^2\left[100\delta(1-\nu) + \bar{\omega}^2\bar{h}^4(\bar{R}+\bar{S})\right]\right\}\right\}\right.\right. \\
&+ 4\bar{h}^2\left\{i^2\pi^2\phi^2\gamma_i^2\left\{m^2\pi^2\left[\nu\bar{h}^2 + 5\delta(1-\nu)\right] + 20\delta\phi^2\bar{\omega}^2(1-\nu)(\bar{R}+\bar{S}+\delta\bar{R}\bar{S}\bar{\omega}^2)\right\}\right. \\
&\left.\left. + \bar{\gamma}_i^2\left\{80\nu\delta\bar{R}\bar{S}\phi^4\bar{\omega}^4 + m^2\pi^2\left[\bar{h}^2 - 5\delta(1-\nu)\right]\left[m^2\pi^2 - 4\phi^2\bar{\omega}^2(\bar{R}+\bar{S})\right]\right\}\right\}\right\}G_m \\
&+ 10i\pi\delta\phi^2\sin\left(\frac{i\pi}{2}\right)\left\{4\gamma_i^2\bar{h}^2\left\{4\left(\xi_i^2 + \eta_i^2\right) - \phi^2\left[i^2\pi^2(2-\nu) + 4\delta\bar{R}\bar{S}\bar{\omega}^4(1-\nu)\right]\right\} + m^2\pi^2\left\{\phi^2\left(40 + \nu i^2\pi^2\bar{h}^2\right) + \left[\bar{h}^2 - 10\delta(1-\nu)\right]\right.\right. \\
&\left.\left.\left.\times\left[4\left(\xi_i^2 + \eta_i^2\right) + \pi^2\left(m^2 - i^2\phi^2\right)\right]\right\}\right\}\bar{H}_m\right\} = 0
\end{aligned} \tag{22}
$$

for $i = 1, 3, 5, \ldots$, where $\bar{F}_i = aF_i/D$, $\bar{H}_m = aH_m/D$, $\xi_i = \phi\sqrt{i^2\pi^2 - 4\bar{R}\bar{\omega}^2}/2$, $\eta_i = \phi\sqrt{i^2\pi^2 - 4\bar{S}\bar{\omega}^2}/2$, $\epsilon_i = i^2\pi^2\bar{h}^2 - 20\delta\bar{R}\bar{\omega}^2$, $\zeta_i = i^2\pi^2\bar{h}^2 - 20\delta\bar{S}\bar{\omega}^2$, $\bar{\epsilon}_i = -4\bar{R}\bar{\omega}^2 - i^2\pi^2(1-\nu)(1+\delta\bar{R}\bar{\omega}^2)$, $\bar{\zeta}_i = -4\bar{S}\bar{\omega}^2 - i^2\pi^2(1-\nu)(1+\delta\bar{S}\bar{\omega}^2)$, $\gamma_i = \phi\sqrt{40/\bar{h}^2 + i^2\pi^2}/2$, and $\bar{\gamma}_i = \phi\sqrt{40/\bar{h}^2 + i^2\pi^2/\phi^2}/2$. Corresponding to condition **(b)**, we have

$$\begin{aligned}
&\phi\gamma_i\left[\delta i^2\pi^2\bar{h}^2\bar{\omega}^2\mathrm{sech}\gamma_i(\bar{R}-\bar{S}) + \epsilon_i\mathrm{sech}\xi_i(1+\delta\bar{S}\bar{\omega}^2) - \zeta_i\mathrm{sech}\eta_i(1+\delta\bar{R}\bar{\omega}^2)\right]E_i \\
&-5\delta\left\{\delta i^2\pi^2\phi^2\bar{\omega}^2\mathrm{th}\,\gamma_i(\bar{R}-\bar{S}) + 4\gamma_i\left[\xi_i\,\mathrm{th}\,\xi_i(1+\delta\bar{S}\bar{\omega}^2) - \eta_i\,\mathrm{th}\,\eta_i(1+\delta\bar{R}\bar{\omega}^2)\right]\right\}\bar{F}_i \\
&+\sum_{m=1,3,5,\ldots}^{\infty}\sin\left(\frac{m\pi}{2}\right)\frac{16m\pi\gamma_i\phi^2\bar{\omega}^2(\bar{R}-\bar{S})}{\left(4\xi_i^2+m^2\pi^2\right)\left(4\eta_i^2+m^2\pi^2\right)\left[40\phi^2+\pi^2\bar{h}^2\left(m^2+i^2\phi^2\right)\right]} \\
&\times\left\{\left\{\pi^2\left\{\pi^2\bar{h}^2m^4\left(\bar{h}^2-5\delta\right) - 5\delta i^2\phi^4\left(40-i^2\pi^2\bar{h}^2\right) - m^2\phi^2\left[200\delta - \bar{h}^2\left(40+i^2\pi^2\bar{h}^2\right)\right]\right\}\right.\right. \\
&\left.-40\delta i^2\pi^2\bar{h}^2\bar{\omega}^2\phi^4(\bar{R}+\bar{S}) - 4\delta\bar{R}\bar{S}\phi^2\left\{m^2\pi^2\bar{h}^2\left(5\delta-\bar{h}^2\right) + 5\phi^2\bar{\omega}^4\left[40\delta - \bar{h}^2(8-\delta i^2\pi^2)\right]\right\}\right\}G_m \\
&\left.+10\delta i\pi\phi^2\sin\left(\frac{i\pi}{2}\right)\left\{\pi^2\left(\bar{h}^2-10\delta\right)\left(m^2+i^2\phi^2\right) + 4\phi^2\left\{10+\delta\bar{\omega}^2\left[\bar{R}\bar{S}\bar{h}^2\bar{\omega}^2 + 10(\bar{R}+\bar{S})\right]\right\}\right\}\bar{H}_m\right\} = 0
\end{aligned} \tag{23}$$

for $i = 1, 3, 5, \ldots$. Corresponding to conditions **(c)** and **(d)**, one just needs to replace a, b, E_i, F_i, G_m, and H_m in Eqs. (22) and (23) with b, a, G_i, H_i, E_m, and F_m, respectively, to yield two more sets of equations. The generated four sets of linear equations with respect to four sets of unknowns E_m, F_m, G_n, and H_n ($m = 1, 3, 5, \ldots$; $n = 1, 3, 5, \ldots$) have nonzero solutions provided that the determinant of the equations' coefficient matrix is zero. Because the frequency parameter $\bar{\omega}$ has been included in the coefficient matrix, the zero-determinant condition will yield an equation with respect to $\bar{\omega}$. The mode shape corresponding to a frequency can be obtained by seeking a set of nonzero solutions for E_m, F_m, G_n, and H_n under one determined $\bar{\omega}$, followed by their substitution into two fundamental problems' solutions and summation. It is worth pointing out that the solution for CCFF plate can reduce to those for CSFF and SSFF plates. Simply deleting the set of equations corresponding to condition **(d)** and setting $H_n = 0$, the solution of a CSFF plate can be obtained. Deleting the equations corresponding to both conditions **(b)** and **(d)** and

Table 1 Frequency parameters, $\omega a^2\sqrt{\rho h/D}$, of CCFF thick plate with $h/a = 0.05$

b/a	Reference	Mode: First	Second	Third	Fourth	Fifth	Sixth	Seventh	Eighth	Ninth	Tenth
1	Present	6.8327	23.418	26.096	45.966	60.760	63.513	81.574	84.255	115.24	117.68
	FEM (shell)	6.8273	23.329	26.011	45.711	60.283	63.045	80.777	83.497	113.73	116.19
	FEM (brick)	6.7010	22.902	25.541	44.908	59.235	61.957	79.401	82.102	111.90	114.34
1.5	Present	4.9237	13.037	22.924	29.544	33.265	50.464	54.552	60.871	70.098	75.256
	FEM (shell)	4.9208	13.013	22.846	29.430	33.131	50.166	54.200	60.420	69.523	74.632
	FEM (brick)	4.8284	12.771	22.427	28.889	32.535	49.277	53.236	59.372	68.323	73.344
2	Present	4.2515	8.9751	18.083	22.415	28.182	32.307	38.637	50.910	53.055	60.380
	FEM (shell)	4.2493	8.9648	18.040	22.342	28.076	32.181	38.460	50.609	52.739	59.935
	FEM (brick)	4.1691	8.7965	17.702	21.931	27.566	31.587	37.768	49.696	51.800	58.895
2.5	Present	3.9523	7.0476	12.870	21.417	22.494	25.911	32.681	34.036	42.358	48.912
	FEM (shell)	3.9503	7.0416	12.848	21.353	22.427	25.819	32.546	33.902	42.149	48.641
	FEM (brick)	3.8756	6.9090	12.607	20.954	22.012	25.347	31.954	33.276	41.390	47.758
3	Present	3.7988	5.9726	10.022	16.151	21.945	24.179	25.018	29.511	34.995	36.435
	FEM (shell)	3.7969	5.9682	10.009	16.119	21.873	24.099	24.940	29.398	34.853	36.277
	FEM (brick)	3.7250	5.8557	9.8200	15.814	21.471	23.652	24.479	28.862	34.207	35.619
3.5	Present	3.7113	5.3112	8.2993	12.784	18.826	21.928	23.833	26.506	27.628	32.634
	FEM (shell)	3.7095	5.3077	8.2907	12.764	18.782	21.856	23.752	26.420	27.530	32.501
	FEM (brick)	3.6392	5.2076	8.1342	12.522	18.427	21.454	23.316	25.925	27.026	31.910
4	Present	3.6574	4.8772	7.1761	10.598	15.219	20.942	21.979	23.365	26.152	28.201
	FEM (shell)	3.6556	4.8742	7.1697	10.584	15.190	20.887	21.910	23.287	26.058	28.109
	FEM (brick)	3.5863	4.7821	7.0340	10.383	14.902	20.493	21.506	22.859	25.581	27.581
4.5	Present	3.6221	4.5787	6.4017	9.1002	12.736	17.326	21.775	22.728	23.260	25.260
	FEM (shell)	3.6202	4.5760	6.3963	9.0899	12.716	17.289	21.704	22.658	23.191	25.172
	FEM (brick)	3.5516	4.4896	6.2756	8.9177	12.474	16.961	21.304	22.236	22.760	24.711
5	Present	3.5977	4.3659	5.8449	8.0294	10.962	14.670	19.138	21.817	22.751	24.296
	FEM (shell)	3.5959	4.3634	5.8407	8.0217	10.947	14.644	19.095	21.745	22.675	24.219
	FEM (brick)	3.5277	4.2809	5.7302	7.8691	10.739	14.365	18.732	21.345	22.259	23.767

Table 2 Frequency parameters, $\omega a^2\sqrt{\rho h/D}$, of CCFF thick plate with $h/a = 0.1$

b/a	Reference	Mode									
		First	Second	Third	Fourth	Fifth	Sixth	Seventh	Eighth	Ninth	Tenth
1	Present	6.6934	22.457	25.010	42.797	56.302	58.768	73.632	76.064	101.95	103.84
	FEM (shell)	6.6727	22.143	24.722	41.999	54.905	57.425	71.452	74.072	98.344	100.33
	FEM (brick)	6.6564	22.106	24.695	41.976	54.929	57.467	71.503	74.173	98.608	100.59
	Liew et al. [30]	6.6738	22.145	24.722	42.002	54.908	57.429	71.455	74.076	98.352	100.34
1.5	Present	4.8528	12.676	22.099	28.300	31.540	46.992	51.080	56.500	64.302	68.664
	FEM (shell)	4.8416	12.589	21.828	27.914	31.097	46.076	50.019	55.191	62.679	66.935
	FEM (brick)	4.8282	12.558	21.797	27.866	31.063	46.047	50.005	55.228	62.726	66.960
	Liew et al. [30]	4.8420	12.591	21.831	27.916	31.099	46.080	50.022	55.196	62.684	66.943
2	Present	4.2047	8.7739	17.547	21.643	26.920	30.947	36.449	47.916	49.428	56.097
	FEM (shell)	4.1958	8.7349	17.392	21.385	26.562	30.526	35.876	46.988	48.468	54.801
	FEM (brick)	4.1840	8.7104	17.348	21.355	26.525	30.472	35.837	46.950	48.440	54.839
	Liew et al. [30]	4.1966	8.7366	17.395	21.386	26.565	30.530	35.880	46.998	48.479	54.809
2.5	Present	3.9162	6.9125	12.554	20.731	21.746	24.851	31.071	32.577	39.858	46.205
	FEM (shell)	3.9083	6.8889	12.477	20.502	21.512	24.535	30.624	32.132	39.194	45.366
	FEM (brick)	3.8973	6.8688	12.440	20.457	21.475	24.501	30.582	32.075	39.152	45.319
	Liew et al. [30]	3.9084	6.8929	12.479	20.506	21.513	24.539	30.629	32.139	39.206	45.384
3	Present	3.7683	5.8725	9.8047	15.727	21.218	23.312	24.119	28.162	33.497	34.519
	FEM (shell)	3.7609	5.8557	9.7578	15.609	20.965	23.032	23.854	27.782	33.026	34.005
	FEM (brick)	3.7504	5.8383	9.7283	15.564	20.935	22.988	23.809	27.743	32.964	33.961
3.5	Present	3.6843	5.2321	8.1359	12.488	18.301	21.204	22.955	25.561	26.478	31.038
	FEM (shell)	3.6771	5.2188	8.1041	12.413	18.145	20.954	22.674	25.262	26.149	30.596
	FEM (brick)	3.6669	5.2032	8.0789	12.375	18.092	20.924	22.641	25.204	26.109	30.553
4	Present	3.6325	4.8119	7.0458	10.373	14.844	20.322	21.263	22.526	25.091	27.192
	FEM (shell)	3.6255	4.8004	7.0221	10.322	14.742	20.125	21.022	22.254	24.771	26.876
	FEM (brick)	3.6154	4.7862	7.0001	10.289	14.696	20.071	20.990	22.223	24.736	26.812
4.5	Present	3.5986	4.5230	6.2937	8.9204	12.450	16.877	21.066	21.979	22.491	24.271
	FEM (shell)	3.5918	4.5127	6.2745	8.8825	12.377	16.747	20.818	21.730	22.256	23.968
	FEM (brick)	3.5818	4.4994	6.2550	8.8536	12.338	16.696	20.787	21.688	22.209	23.933
5	Present	3.5754	4.3170	5.7528	7.8799	10.733	14.324	18.619	21.104	21.965	23.451
	FEM (shell)	3.5685	4.3076	5.7367	7.8502	10.679	14.230	18.463	20.855	21.701	23.176
	FEM (brick)	3.5587	4.2949	5.7190	7.8251	10.644	14.184	18.407	20.826	21.671	23.130

Table 3 Frequency parameters, $\omega a^2\sqrt{\rho h/D}$, of CCFF thick plate with $h/a = 0.2$

b/a	Reference	Mode									
		First	Second	Third	Fourth	Fifth	Sixth	Seventh	Eighth	Ninth	Tenth
1	Present	6.3126	19.806	21.921	35.427	45.438	47.208	57.159	58.733	75.425	76.528
	FEM (shell)	6.2445	18.969	21.218	33.770	42.900	44.939	53.567	55.802	70.541	72.030
	FEM (brick)	6.2661	19.073	21.367	34.014	43.313	45.394	54.074	56.407	71.434	72.929
	Liew et al. [30]	6.2455	18.970	21.219	33.771	42.901	44.939	53.568	55.802	70.545	72.034
1.5	Present	4.6522	11.656	19.622	24.806	27.085	38.794	42.131	45.624	50.999	54.149
	FEM (shell)	4.6132	11.392	18.919	23.855	26.076	36.982	40.146	43.332	48.292	51.343
	FEM (brick)	4.6269	11.434	19.040	23.992	26.254	37.256	40.492	43.776	48.783	51.827
	Liew et al. [30]	4.6140	11.392	18.920	23.857	26.077	36.983	40.148	43.333	48.293	51.345
2	Present	4.0663	8.2084	15.989	19.259	23.483	27.073	30.945	40.013	40.747	45.352
	FEM (shell)	4.0351	8.0814	15.551	18.585	22.604	26.090	29.693	38.206	38.939	43.079
	FEM (brick)	4.0471	8.1059	15.612	18.707	22.748	26.242	29.895	38.495	39.249	43.524
	Liew et al. [30]	4.0357	8.0822	15.553	18.586	22.605	26.091	29.694	38.208	38.941	43.081
2.5	Present	3.8050	6.5320	11.644	18.658	19.465	21.842	26.817	28.439	33.622	38.899
	FEM (shell)	3.7769	6.4535	11.405	18.019	18.875	21.051	25.773	27.428	32.223	37.273
	FEM (brick)	3.7883	6.4711	11.440	18.114	18.981	21.186	25.938	27.590	32.446	37.550
	Liew et al. [30]	3.7771	6.4537	11.406	18.020	18.877	21.052	25.773	27.430	32.225	37.277
3	Present	3.6711	5.5888	9.1833	14.478	18.930	20.719	21.523	24.508	29.179	29.604
	FEM (shell)	3.6445	5.5315	9.0327	14.134	18.265	19.973	20.877	23.588	28.067	28.507
	FEM (brick)	3.6557	5.5462	9.0572	14.181	18.386	20.092	20.984	23.739	28.237	28.688
3.5	Present	3.5951	5.0061	7.6700	11.621	16.740	18.915	18.915	22.733	23.311	26.814
	FEM (shell)	3.5694	4.9598	7.5643	11.393	16.300	18.258	19.612	21.927	22.562	25.781
	FEM (brick)	3.5806	4.9730	7.5832	11.425	16.358	18.381	19.741	22.046	22.689	25.947
4	Present	3.5486	4.6230	6.6748	9.7216	13.735	18.441	19.018	19.989	22.067	24.213
	FEM (shell)	3.5234	4.5831	6.5942	9.5586	13.432	17.870	18.416	19.288	21.266	23.421
	FEM (brick)	3.5345	4.5955	6.6105	9.5825	13.472	17.953	18.525	19.415	21.403	23.535
4.5	Present	3.5182	4.3595	5.9859	8.4021	11.609	15.534	18.817	19.631	20.237	21.405
	FEM (shell)	3.4934	4.3235	5.9210	8.2787	11.386	15.162	18.161	18.944	19.657	20.640
	FEM (brick)	3.5045	4.3355	5.9354	8.2982	11.416	15.210	18.281	19.063	19.746	20.773
5	Present	3.4974	4.1716	5.4898	7.4506	10.063	13.293	17.058	18.837	19.537	20.832
	FEM (shell)	3.4728	4.1384	5.4347	7.3526	9.8916	13.012	16.621	18.184	18.851	20.088
	FEM (brick)	3.4840	4.1501	5.4482	7.3695	9.9155	13.049	16.677	18.306	18.978	20.214

Table 4 Frequency parameters, $\omega a^2\sqrt{\rho h/D}$, of CSFF thick plate with $h/a = 0.2$

b/a	Reference	Mode First	Second	Third	Fourth	Fifth	Sixth	Seventh	Eighth	Ninth	Tenth
1	Present	4.9666	16.927	20.685	33.556	42.155	46.323	55.319	57.284	73.039	75.829
	FEM (shell)	4.9173	16.272	19.955	31.981	39.667	43.944	51.915	54.187	68.160	71.088
	FEM (brick)	4.9290	16.302	20.041	32.151	39.880	44.368	52.287	54.694	68.771	71.829
	Liew et al. [30]	4.9180	16.272	19.956	31.981	39.667	43.944	51.916	54.188	68.162	71.088
1.5	Present	2.9049	10.885	15.627	23.925	24.933	37.187	41.090	42.351	47.771	53.234
	FEM (shell)	2.8846	10.638	15.077	22.947	24.065	35.443	38.741	40.368	45.046	50.461
	FEM (brick)	2.8877	10.667	15.100	23.029	24.199	35.645	38.959	40.700	45.335	50.883
	Liew et al. [30]	2.8849	10.638	15.077	22.948	24.066	35.444	38.741	40.369	45.047	50.462
2	Present	2.0272	7.1681	14.762	15.825	20.290	26.774	28.699	39.103	39.831	41.310
	FEM (shell)	2.0151	7.0610	14.253	15.389	19.536	25.793	27.532	37.272	37.930	39.151
	FEM (brick)	2.0160	7.0719	14.275	15.437	19.587	25.933	27.653	37.489	38.190	39.403
	Liew et al. [30]	2.0154	7.0617	14.254	15.391	19.536	25.794	27.533	37.273	37.932	39.151
2.5	Present	1.5456	5.2678	10.906	14.806	18.126	18.907	24.140	28.149	31.626	38.693
	FEM (shell)	1.5369	5.2086	10.685	14.285	17.478	18.356	23.203	27.140	30.297	37.031
	FEM (brick)	1.5371	5.2130	10.708	14.302	17.518	18.423	23.279	27.291	30.438	37.293
	Liew et al. [30]	1.5367	5.2092	10.686	14.285	17.478	18.357	23.203	27.141	30.298	37.036
3	Present	1.2441	4.1403	8.2748	13.800	17.160	20.898	21.565	27.066	29.074	33.709
	FEM (shell)	1.2373	4.1022	8.1436	13.442	16.544	20.231	20.803	25.983	28.042	32.272
	FEM (brick)	1.2372	4.1039	8.1547	13.471	16.573	20.304	20.868	26.082	28.198	32.432
3.5	Present	1.0390	3.4002	6.6014	10.899	14.584	16.153	16.667	19.743	22.659	24.143
	FEM (shell)	1.0335	3.3731	6.5150	10.688	14.074	15.645	16.175	19.014	21.961	23.219
	FEM (brick)	1.0332	3.3734	6.5208	10.707	14.090	15.676	16.218	19.058	22.054	23.294
4	Present	0.89116	2.8794	5.4641	8.8735	13.101	14.604	15.988	18.157	18.685	22.074
	FEM (shell)	0.88649	2.8585	5.4032	8.7292	12.806	14.102	15.423	17.611	18.070	21.240
	FEM (brick)	0.88617	2.8583	5.4058	8.7404	12.833	14.119	15.446	17.658	18.119	21.299
4.5	Present	0.77980	2.4941	4.6487	7.4324	10.895	14.450	15.078	15.729	17.757	19.766
	FEM (shell)	0.77578	2.4773	4.6030	7.3281	10.690	13.957	14.684	15.199	17.118	19.203
	FEM (brick)	0.77541	2.4768	4.6041	7.3344	10.708	13.974	14.718	15.225	17.151	19.268
5	Present	0.69303	2.1983	4.0389	6.3681	9.2496	12.660	14.528	15.425	16.635	17.209
	FEM (shell)	0.68945	2.1843	4.0031	6.2895	9.0974	12.392	14.024	14.882	16.193	16.623
	FEM (brick)	0.68910	2.1835	4.0032	6.2928	9.1084	12.416	14.041	14.903	16.234	16.657

Table 5 Frequency parameters, $\omega a^2\sqrt{\rho h/D}$, of SSFF thick plate with $h/a = 0.2$

b/a	Reference	Mode First	Second	Third	Fourth	Fifth	Sixth	Seventh	Eighth	Ninth	Tenth
1	Present	3.2081	15.787	17.510	31.590	41.359	42.960	54.182	55.152	72.478	73.642
	FEM (shell)	3.1797	15.158	16.918	30.099	38.797	40.610	50.777	52.093	67.463	68.977
	FEM (brick)	3.1767	15.167	16.945	30.186	38.981	40.840	51.072	52.436	68.044	69.584
	Liew et al. [30]	3.1800	15.158	16.917	30.099	38.797	40.610	50.777	52.093	67.462	68.977
1.5	Present	2.1459	8.9337	15.414	21.730	23.418	35.723	39.164	41.517	47.414	51.605
	FEM (shell)	2.1318	8.7475	14.861	20.881	22.516	34.025	37.122	39.222	44.675	48.861
	FEM (brick)	2.1297	8.7475	14.877	20.928	22.571	34.159	37.314	39.439	44.938	49.175
	Liew et al. [30]	2.1318	8.7474	14.861	20.881	22.517	34.025	37.122	39.222	44.675	48.861
2	Present	1.6018	6.0129	13.524	15.127	19.795	24.659	27.801	37.755	38.079	41.169
	FEM (shell)	1.5924	5.9297	13.140	14.617	19.051	23.727	26.651	35.969	36.295	38.867
	FEM (brick)	1.5908	5.9275	13.152	14.636	19.085	23.802	26.733	36.146	36.473	39.082
	Liew et al. [30]	1.5920	5.9297	13.140	14.618	19.05	23.728	26.652	35.969	36.295	38.867
2.5	Present	1.2746	4.5144	9.6482	14.732	17.047	18.126	23.570	26.437	30.835	37.046
	FEM (shell)	1.2675	4.4670	9.4575	14.210	16.525	17.494	22.646	25.456	29.524	35.410
	FEM (brick)	1.2662	4.4643	9.4611	14.226	16.553	17.525	22.702	25.549	29.631	35.600
	Liew et al. [30]	1.2673	4.4670	9.4580	14.210	16.525	17.494	22.646	25.456	29.525	35.415
3	Present	1.0574	3.6112	7.3749	12.671	14.707	16.974	19.585	21.131	26.491	27.653
	FEM (shell)	1.0517	3.5797	7.2615	12.367	14.197	16.362	18.980	20.346	25.421	26.639
	FEM (brick)	1.0506	3.5771	7.2614	12.379	14.214	16.386	19.025	20.391	25.497	26.746
3.5	Present	0.90326	3.0086	5.9339	9.9803	14.489	15.275	16.393	19.475	21.467	23.731
	FEM (shell)	0.89850	2.9855	5.8590	9.7898	13.990	14.862	15.822	18.754	20.793	22.816
	FEM (brick)	0.89755	2.9830	5.8574	9.7949	14.005	14.885	15.846	18.790	20.852	22.876
4	Present	0.78828	2.5782	4.9517	8.1529	12.229	14.569	15.890	17.236	18.431	21.763
	FEM (shell)	0.78420	2.5601	4.8982	8.0224	11.959	14.061	15.326	16.761	17.770	20.938
	FEM (brick)	0.78335	2.5579	4.8960	8.0242	11.971	14.077	15.347	16.795	17.803	20.987
4.5	Present	0.69929	2.2558	4.2439	6.8571	10.172	14.059	14.648	15.638	17.606	18.878
	FEM (shell)	0.69567	2.2410	4.2034	6.7626	9.9815	13.675	14.182	15.091	16.970	18.344
	FEM (brick)	0.69494	2.2389	4.2010	6.7624	9.9880	13.691	14.201	15.112	16.999	18.388
5	Present	0.62838	2.0053	3.7114	5.9004	8.6514	11.961	14.501	15.348	15.921	17.076
	FEM (shell)	0.62517	1.9927	3.6793	5.8288	8.5106	11.711	13.995	14.814	15.507	16.471
	FEM (brick)	0.62449	1.9908	3.6769	5.8275	8.5134	11.723	14.011	14.834	15.535	16.497

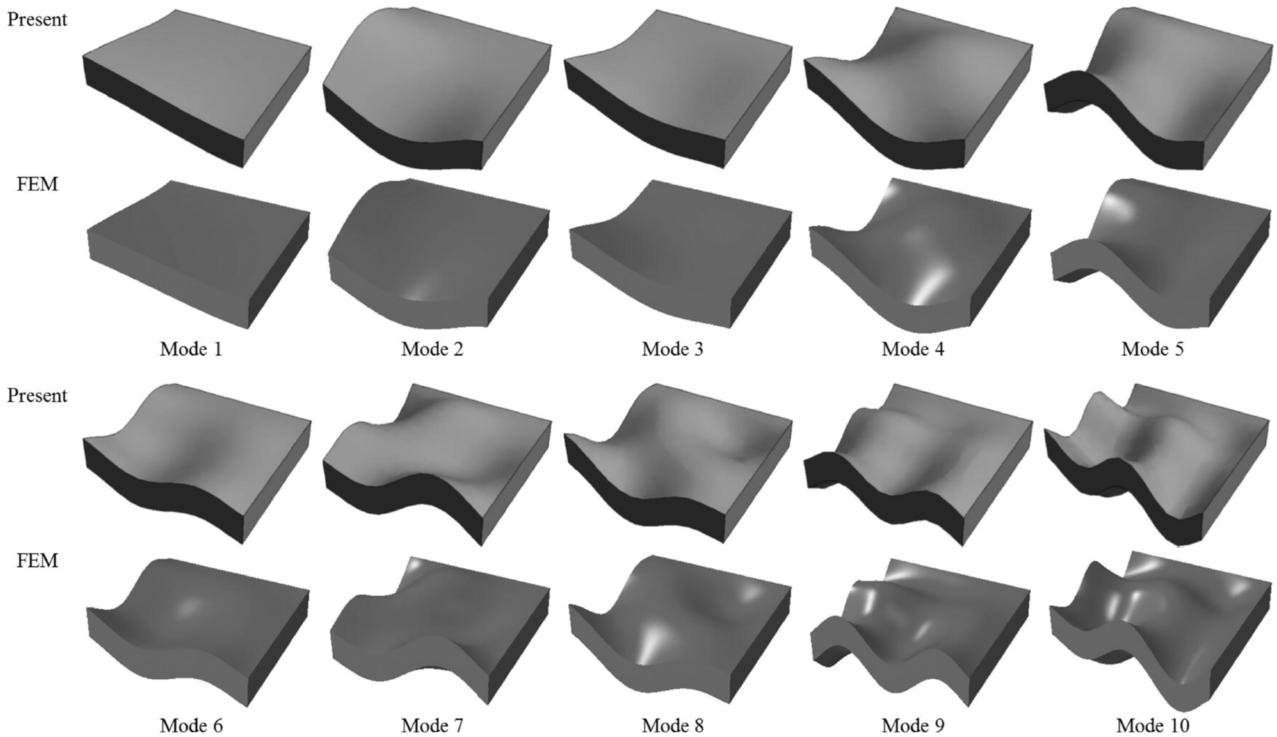

Fig. 2 First ten mode shapes of a CCFF square thick plate with $h/a = 0.2$

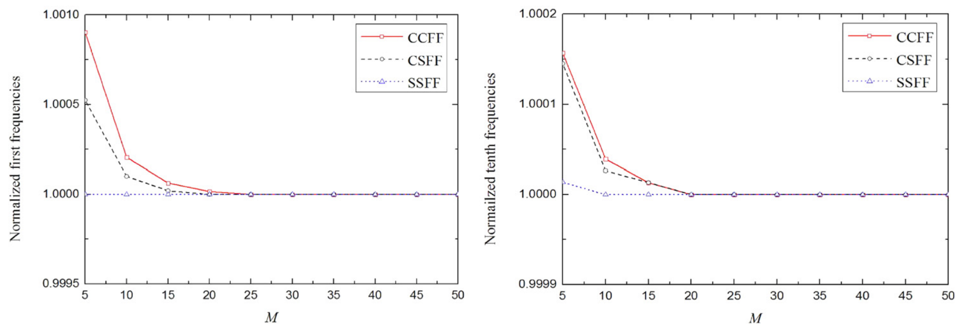

Fig. 3 Convergence of the first and tenth normalized frequencies for CCFF, CSFF, and SSFF square plates with $h/a = 0.2$

setting both $F_m = 0$ and $H_n = 0$, we obtain the solution of a SSFF plate.

4 Comprehensive Numerical and Graphic Results

To provide comprehensive natural frequency and mode shape solutions, we present many numerical and graphic results. In Tables 1–3, we tabulate the first ten natural frequencies of CCFF plates with the aspect ratio b/a ranging from 1 to 5 under an interval of 0.5. The thickness-to-width ratio h/a is set to be 0.05, 0.1, and 0.2, respectively. Tables 4 and 5 correspond to CSFF and SSFF plates, respectively, with $h/a = 0.2$ and b/a being the same as those for Tables 1–3. The Poisson's ratio 0.3 is adopted throughout. All our analytic solutions are compared with their counterparts from the FEM via the ABAQUS software, in which both thick shell element S8R and linear brick element C3D8R are adopted [29]. Some numerical solutions by the Rayleigh–Ritz method in Ref. [30] are also listed for comparison. Figure 2 illustrates the mode shapes of thick enough ($h/a = 0.2$) square CCFF plates, from both our analytic and finite element solutions. A total of 450 frequencies (90 per table) and ten mode shapes are presented for benchmark purpose, all of which are well validated by satisfactory agreement with the FEM and Ref. [30]. It should be noted that the minor differences between the present solutions and both the FEM and Ref. [30] increase for higher modes, which seems more obvious for thicker plates. This is probably due to the difference between the present plate theory neglecting the rotatory inertia and that incorporating the rotatory inertia (Ref. [30] and FEM with thick shell element) as well as three-dimensional elasticity (FEM with linear brick element).

The convergence study is carried out by plotting the first and tenth frequency solutions of the CCFF, CSFF, and SSFF square plates with $h/a = 0.2$, normalized by their convergent values, versus the number of series terms (specified throughout as M in this study), as shown in Fig. 3. It is verified that only 50 terms are adequate for achieving the accuracy of five significant figures for all current solutions; thus, $M = 50$ is universally applied to yield the results.

5 Conclusions

New analytic free vibration solutions are obtained for the rectangular thick plates with a free corner based on the symplectic superposition method, including CCFF, CSFF, and SSFF plates.

The governing equations are first transformed into the Hamiltonian system, where the effective mathematical techniques in the symplectic space such as the variable separation and symplectic eigen expansion are valid. A problem to be solved is treated as the sum of two fundamental problems that can be analytically solved with the above techniques. The equivalence between the original problem and the sum of fundamental problems leads to an equation to determine the frequencies. The mode shapes are then obtained without difficulty. The main advantage of the method is its ability to yield analytic solutions in a rational and rigorous way, without loss of fast convergence and accuracy. Comprehensive numerical and graphic results will play an important role in validating other new solution methods as the benchmarks.

Funding Data

- Young Elite Scientist Sponsorship Program by CAST (No. 2015QNRC003).
- National Basic Research Program of China (Grant No. 2014CB046506).
- National Natural Science Foundation of China (Grant Nos. 11302038, 11572323, and 11772331).
- Strategic Priority Research Program of the Chinese Academy of Sciences (No. XDB22040501).
- State Key Laboratory of Structural Analysis for Industrial Equipment, Dalian University of Technology (No. GZ1603).
- State Key Laboratory of Digital Manufacturing Equipment and Technology, Huazhong University of Science and Technology (No. DMETKF2017008).

References

[1] Leissa, A. W., 1969, *Vibration of Plates, Office of Technology Utilization*, NASA, Washington, DC.
[2] Reissner, E., 1945, "The Effect of Transverse Shear Deformation on the Bending of Elastic Plates," ASME J. Appl. Mech., **12**(2), pp. A69–A77.
[3] Mindlin, R. D., 1951, "Influence of Rotatory Inertia and Shear on Flexural Motions of Isotropic, Elastic Plates," ASME J. Appl. Mech., **18**(1), pp. 31–38.
[4] Reddy, J. N., 1984, "A Simple Higher-Order Theory for Laminated Composite Plates," ASME J. Appl. Mech., **51**(4), pp. 745–752.
[5] Reddy, J. N., 1984, "A Refined Nonlinear-Theory of Plates With Transverse-Shear Deformation," Int. J. Solids Struct., **20**(9–10), pp. 881–896.
[6] Wu, K., and Zhu, W., 2018, "A New Global Spatial Discretization Method for Calculating Dynamic Responses of Two-Dimensional Continuous Systems With Application to a Rectangular Kirchhoff Plate," ASME J. Vib. Acoust., **140**(1), p. 011002.
[7] Wang, C. Y., 2015, "Vibrations of Completely Free Rounded Rectangular Plates," ASME J. Vib. Acoust., **137**(2), p. 024502.
[8] Leamy, M. J., 2016, "Semi-Exact Natural Frequencies for Kirchhoff-Love Plates Using Wave-Based Phase Closure," ASME J. Vib. Acoust., **138**(2), p. 021008.
[9] Waksmanski, N., Pan, E., Yang, L.-Z., and Gao, Y., 2014, "Free Vibration of a Multilayered One-Dimensional Quasi-Crystal Plate," ASME J. Vib. Acoust., **136**(4), p. 041019.
[10] Lai, S. K., and Xiang, Y., 2012, "Buckling and Vibration of Elastically Restrained Standing Vertical Plates," ASME J. Vib. Acoust., **134**(1), p. 014502.
[11] Malekzadeh, P., and Karami, G., 2004, "Vibration of Non-Uniform Thick Plates on Elastic Foundation by Differential Quadrature Method," Eng. Struct., **26**(10), pp. 1473–1482.
[12] Cho, D. S., Kim, B. H., Kim, J. H., Vladimir, N., and Choi, T. M., 2015, "Forced Vibration Analysis of Arbitrarily Constrained Rectangular Plates and Stiffened Panels Using the Assumed Mode Method," Thin-Walled Struct., **90**, pp. 182–190.
[13] Zhou, D., Cheung, Y. K., Au, F. T. K., and Lo, S. H., 2002, "Three-Dimensional Vibration Analysis of Thick Rectangular Plates Using Chebyshev Polynomial and Ritz Method," Int. J. Solids Struct., **39**(26), pp. 6339–6353.
[14] Pradhan, K. K., and Chakraverty, S., 2015, "Transverse Vibration of Isotropic Thick Rectangular Plates Based on New Inverse Trigonometric Shear Deformation Theories," Int. J. Mech. Sci., **94–95**, pp. 211–231.
[15] Ye, T., Jin, G., Su, Z., and Chen, Y., 2014, "A Modified Fourier Solution for Vibration Analysis of Moderately Thick Laminated Plates With General Boundary Restraints and Internal Line Supports," Int. J. Mech. Sci., **80**, pp. 29–46.
[16] Jin, G., Su, Z., Shi, S., Ye, T., and Gao, S., 2014, "Three-Dimensional Exact Solution for the Free Vibration of Arbitrarily Thick Functionally Graded Rectangular Plates With General Boundary Conditions," Compos. Struct., **108**, pp. 565–577.
[17] Zhang, H., Shi, D., and Wang, Q., 2017, "An Improved Fourier Series Solution for Free Vibration Analysis of the Moderately Thick Laminated Composite Rectangular Plate With Non-Uniform Boundary Conditions," Int. J. Mech. Sci., **121**, pp. 1–20.
[18] Li, R., Wang, P., Tian, Y., Wang, B., and Li, G., 2015, "A Unified Analytic Solution Approach to Static Bending and Free Vibration Problems of Rectangular Thin Plates," Sci. Rep., **5**, p. 17054.
[19] Li, R., Tian, Y., Wang, P., Shi, Y., and Wang, B., 2016, "New Analytic Free Vibration Solutions of Rectangular Thin Plates Resting on Multiple Point Supports," Int. J. Mech. Sci., **110**, pp. 53–61.
[20] Wang, B., Li, P., and Li, R., 2016, "Symplectic Superposition Method for New Analytic Buckling Solutions of Rectangular Thin Plates," Int. J. Mech. Sci., **119**, pp. 432–441.
[21] Xing, Y., and Liu, B., 2009, "Characteristic Equations and Closed-Form Solutions for Free Vibrations of Rectangular Mindlin Plates," Acta Mech. Solida Sin., **22**(2), pp. 125–136.
[22] Xing, Y., and Liu, B., 2009, "Closed Form Solutions for Free Vibrations of Rectangular Mindlin Plates," Acta Mech. Sin., **25**, pp. 689–698.
[23] Li, R., Wang, P., Xue, R., and Guo, X., 2017, "New Analytic Solutions for Free Vibration of Rectangular Thick Plates With an Edge Free," Int. J. Mech. Sci., **131–132**, pp. 179–190.
[24] Yao, W., Zhong, W., and Lim, C. W., 2009, *Symplectic Elasticity*, World Scientific, Singapore.
[25] Lim, C. W., and Xu, X. S., 2010, "Symplectic Elasticity: Theory and Applications," ASME Appl. Mech. Rev., **63**(5), p. 050802.
[26] Lim, C. W., Lu, C. F., Xiang, Y., and Yao, W., 2009, "On New Symplectic Elasticity Approach for Exact Free Vibration Solutions of Rectangular Kirchhoff Plates," Int. J. Eng. Sci., **47**(1), pp. 131–140.
[27] Lim, C. W., 2010, "Symplectic Elasticity Approach for Free Vibration of Rectangular Plates," J. Vib. Eng. Technol., **9**(2), pp. 159–163.
[28] Li, R., Zhong, Y., and Li, M., 2013, "Analytic Bending Solutions of Free Rectangular Thin Plates Resting on Elastic Foundations by a New Symplectic Superposition Method," Proc. R. Soc. A-Math. Phys. Eng. Sci., **469**(2153), p. 20120681.
[29] ABAQUS, 2013, *Analysis User's Guide V6.13*, Dassault Systèmes, Pawtucket, RI.
[30] Liew, K. M., Xiang, Y., and Kitipornchai, S., 1993, "Transverse Vibration of Thick Rectangular Plates—1. Comprehensive Sets of Boundary Conditions," Comput. Struct., **49**(1), pp. 1–29.